PAPER Special Section on Recent Progress in Antennas and Propagation in Conjunction with Main Topics of ISAP2012

Compact Antenna Arrangement for MIMO Sensor in Indoor Environment

Naoki HONMA[†a)], ***Member***, **Kentaro NISHIMORI**[††], ***Senior Member***, **Hiroaki SATO**[†], ***and*** **Yoshitaka TSUNEKAWA**[†], ***Members***

SUMMARY This paper proposes the antenna arrangement for 2×2 MIMO (Multiple-Input Multiple-Output) sensor and evaluates the detection performance based on raytracing simulation. In this arrangement, the transmitting and receiving antennas are placed closely. Two types of the arrangement are considered. In the first method, all of the transmitting and receiving antennas are located closely. In the second method, two sets of the antennas are placed separately, and each set has one transmitting and one receiving antennas. The numerical analysis of the indoor propagation based on the raytracing method is carried out. The path distribution and intrusion detection performance with the various antenna arrangements are evaluated for the human positions all over the room. The numerical analysis results show that the proposed antenna arrangements achieve the compact configuration of the sensor antenna system as well as high detection performance.

key words: *MIMO sensor, antenna, element spacing*

1. Introduction

Intrusion sensors using microwave for security application has been studied [1]–[6], in these days. The microwave sensors using existing signals, such as wireless LAN, TV broadcast signals and so on, have been studied, and they have proven that the microwave sensor are effective in break-in detection [1]–[4]. In [2] and [3], the intrusion is detected by observing the amplitude of the received signal, and it is shown that motion of the human body yields change in the reception power of the broadcast signals. The work [4] has proposed the detection algorithm where the eigenvector at the receiving array antennas is exploited to obtain high sensitivity. These microwave sensors can detect the intrusion even when the intruder is at the NLOS (Non Line-Of-Sight) locations, and this is the most attractive feature compared to the other sensors [5].

The authors have studied MIMO (Multiple-Input Multiple-Output) sensor that uses the MIMO channel variation to detect the intruders [5], [6] for indoor environment. The MIMO sensor detects the intrusion by comparing the varying channel with the person to the static one. In [5], the relationship between the antenna height and the detection rate has been studied, and it is found that the antenna needs to be lower than the height of the intruder. In [6] and [7], the effect of the antenna element spacing on the detection rate has been investigated, and two types of the antenna configuration, i.e., SIMO (Single-Input Multiple-Output) and MIMO arrays, are compared. This work indicated that MIMO configuration outperforms SIMO configuration, but large antenna aperture is needed to achieve high sensitivity. The work [8] experimentally explored the effect of antenna diversity, frequency band, and size of the room on the detection rate. In [9], the channel characteristics are evaluated and the effect of the direct path existence and location of the intruder on detection performance was investigated. In these studies, the transmitting and receiving arrays are placed separately at the ends of the rooms. It was found that the arrays with wide antenna spacing are desirable for the high detection performances. In terms of the realistic hardware of the sensor, the excessively large antenna configuration and high hardware complexity are not desirable. Therefore, the efficient antenna arrangement is needed even when the size and number of the antennas are limited.

In this paper, we propose the antenna arrangement for the MIMO sensor where the transmitting and receiving antennas are placed together [10]. The arrangement requires the less antenna spaces than the conventional one. The path distribution and the detection probabilities are evaluated based on the raytrace simulation. It is shown that the proposed antenna arrangement can achieve the fairly high detection performance.

2. Concept of MIMO Sensor and Detection Method

Before discussing the proposed antenna arrangement, the basic concept of the MIMO sensor is explained briefly. Figure 1 is the conceptual sketch of MIMO sensor. This system has M_t transmitting and M_r receiving antennas. At first, the MIMO channel without a person is measured in advance. This channel is static and defined as,

$$\boldsymbol{H}_{no} = \begin{pmatrix} h_{no,11} & \cdots & h_{no,1M_t} \\ \vdots & \ddots & \vdots \\ h_{no,M_r1} & \cdots & h_{no,M_rM_t} \end{pmatrix}. \quad (1)$$

On the other hand, the channel with a person is defined as

$$\boldsymbol{H}_{ob} = \begin{pmatrix} h_{ob,11} & \cdots & h_{ob,1M_t} \\ \vdots & \ddots & \vdots \\ h_{ob,M_r1} & \cdots & h_{ob,M_rM_t} \end{pmatrix}. \quad (2)$$

Manuscript received January 17, 2013.
Manuscript revised May 20, 2013.

[†]The authors are with Iwate University, Morioka-shi, 020-8551 Japan.
[††]The author is with Niigata University, Niigata-shi, 950-2181 Japan.
a) E-mail: honma@iwate-u.ac.jp

DOI: 10.1587/transcom.E96.B.2491

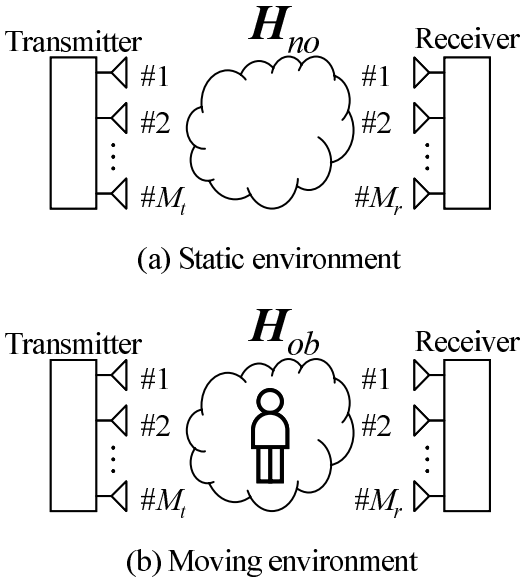

Fig. 1 Concept of MIMO sensor.

The channels, $\boldsymbol{H}_{no}$ and $\boldsymbol{H}_{ob}$, are compared by the evaluation function,

$$\rho = \frac{\left|\sum_{i=1}^{Mr}\sum_{j=1}^{Mt} h_{no,ij}^{*} h_{ob,ij}\right|}{\sqrt{\sum_{i=1}^{Mr}\sum_{j=1}^{Mt}\left|h_{no,ij}\right|^2}\sqrt{\sum_{i=1}^{Mr}\sum_{j=1}^{Mt}\left|h_{ob,ij}\right|^2}}. \tag{3}$$

Now, (3) is defined as channel correlation in this study [6]. This value is lowered when these two channels differ greatly, and approaches to 1 when two channels are identical. Meanwhile, the estimated channel contains the random errors because of the existence of the noise, and the actually observed channel correlation is lower than 1 even when the channel is not varied. In this system, the training symbols known to the receiver are sent from the transmitting antennas. A series of the training signals is defined as $\boldsymbol{S} = [\boldsymbol{s}_1, \cdots, \boldsymbol{s}_{N_S}]$, where N_S is the number of training symbols, $N_S \geq M_t$ and $\boldsymbol{s}_i = [s_{1i}, ..., s_{M_t i}]^T$. The received noise is also defined as $\boldsymbol{N} = [\boldsymbol{n}_1, \cdots, \boldsymbol{n}_{N_S}]$, where $\boldsymbol{n}_i = [n_{1i}, ..., n_{M_r i}]^T$. They satisfy the conditions,

$$\boldsymbol{S}\boldsymbol{S}^H = \frac{N_S P}{M_t}\boldsymbol{I}_{M_t \times M_t} \tag{4}$$

$$E\left[\boldsymbol{N}\boldsymbol{N}^H\right] = N_S \sigma_n^2 \boldsymbol{I}_{M_r \times M_r}, \tag{5}$$

where P is the sum of the transmitted power. The noise is to be zero-mean Gaussian white, and its mean power is σ_n^2. In this case, the estimated channel without any persons at the certain moment is expressed as $\boldsymbol{H}' = \boldsymbol{H}_{no} + \boldsymbol{H}_w$, where $\boldsymbol{H}_w$ is the error component of the estimated channel. Based on the LS (Least Square) estimation, its characteristics can be expressed as,

$$E\left[\boldsymbol{H}_w \boldsymbol{H}_w^H\right] = \frac{\sigma_n^2 M_t^2}{N_S P}\boldsymbol{I}_{M_r \times M_r}. \tag{6}$$

Thus, the power of the error component is decreased in inverse proportion to the training times, N_S.

In the simulation, the transmitting power is $P = 1$ W, the number of the transmitting and receiving antennas are $M_t = M_r = 2$, and the number of the training symbols is set to $N_S = 8$. The static channel, $\boldsymbol{H}_{no}$, is assumed to be obtained accurately by many training rounds, and does not contain noise components. $\boldsymbol{H}_w$ is a Gaussian random matrix, and its variance is determined so as to satisfy (6). The estimation error, $\boldsymbol{H}_w$, is used for considering sensitivity of MIMO sensor. In order to detect the intrusion, the correlation value needs to be observed and the detection is made when the correlation is lower than the certain value. We define a threshold value, ρ_t, and the intrusion is detected when $\rho < \rho_t$. When the estimated channel contains a strong estimation error, the channel correlation is lowered and this yields the false detection. Therefore, ρ_t needs to be sufficiently small so as to reduce the false detection. The threshold value, ρ_t, can be determined by comparing $\boldsymbol{H}_{no}$ and $\boldsymbol{H}_{no} + \boldsymbol{H}_w$, and is given so that the false detection probability becomes 1% in the static environment.

3. Proposed Antenna Arrangement and Numerical Analysis Model

3.1 Antenna Arrangement

The MIMO sensor dealt with in this paper comprises 2×2 vertical dipoles. Figure 2(a) indicates the proposed antenna arrangement. The transmitting and receiving antennas are arranged vertically each other, and this yields small mutual coupling between the transmitting and receiving antennas. Two sets of such antennas are arranged horizontally. The advantage of this arrangement is that the configuration of the sensor system becomes very compact since all of the antennas are placed closely if the horizontal distance between two sets is within some wavelengths.

The arrangement in Fig. 2(b) is another proposal. One set of the transmitting and receiving antennas is placed at one side of the room, and another identical set is placed at another side of the room. As it can be seen in Fig. 2(b), this configuration can cover all over the room even around the corner of the room, which have been dead zone of the MIMO sensor in the previous work [6] if the 4 antennas are placed to 4 corners.

Figure 2(c) shows the antenna arrangement C, which is the conventional one. The transmitting and receiving arrays are located at both ends of the room. This arrangement is normally used in MIMO systems, and this has been well studied in our previous works [5]–[8].

3.2 Numerical Analysis Model

In this study, the detection performance is evaluated using the raytracing simulation based on the imaging method. Figure 3 shows the numerical analysis model for indoor environment. Two different environments are tested in this study.

One is a small room, whose dimension is $W_x \times W_y \times W_z = 7.8 \times 6.8 \times 2.5\ \mathrm{m}^3$. The other is a large room, whose dimension is $15.6 \times 13.6 \times 2.5\ \mathrm{m}^3$. The materials of wall, ceiling, and floor are assumed to be concrete (the relative permittivity: 6.0). The human body is approximated as the rectangular dielectrics whose dimension is $0.2 \times 0.34 \times 1.7\ \mathrm{m}^3$ (the relative permittivity: 37.5), and it is placed at the position (x, y). The height of the antenna, h, the antenna spacing, d, and positions are mentioned in the following section. In the raytracing simulation, the number of the maximum reflection times is set to 5. The number of the human body is 1, and the human body is moved with 0.5 m step and 1.0 m step in xy directions for the small and large rooms, respectively, i.e., 180 positions are evaluated for each environment. The frequency is 2.4 GHz or 5.2 GHz, and the bandwidth is 10 MHz. The dipole radiation pattern is used, but the mutual coupling is neglected for simplicity.

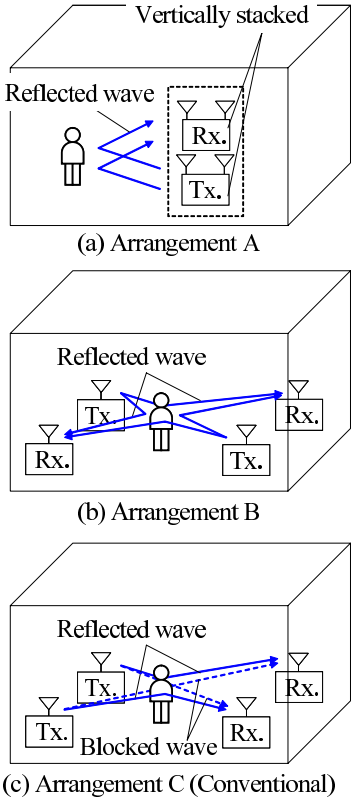

Fig. 2 Antenna arrangement: (a) Arrangement A (Proposed), (b) Arrangement B (Proposed), (c) Arrangement C (Conventional).

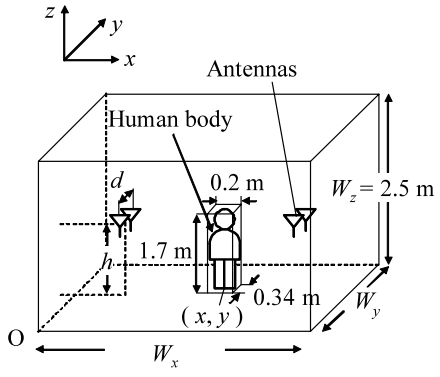

Fig. 3 Analysis model.

4. Results

Figure 4 shows the path distribution calculated by imaging method. Figures 4(a), (b) and (c) corresponds to the arrangements A, B, and C, respectively. Here, the distributions are projected onto xy-plane. The position of human body is set to $(x, y) = (3.9, 3.4)$ m, and the antenna height is set to $h = 1.0$ m. In the arrangement A, the antennas are located on the plane, $X = 3.9$ m. In the arrangements B and C, the antennas are located on the planes, $X = 0.6$ m, $X = 7.6$ m. The antenna spacing, d, is set to $0.5\lambda_0$ (λ_0: wavelength in vacuum). For simplicity, only the major paths are shown in these figures. It can be seen that the arrangement A yields radial path distributions. However, the relatively

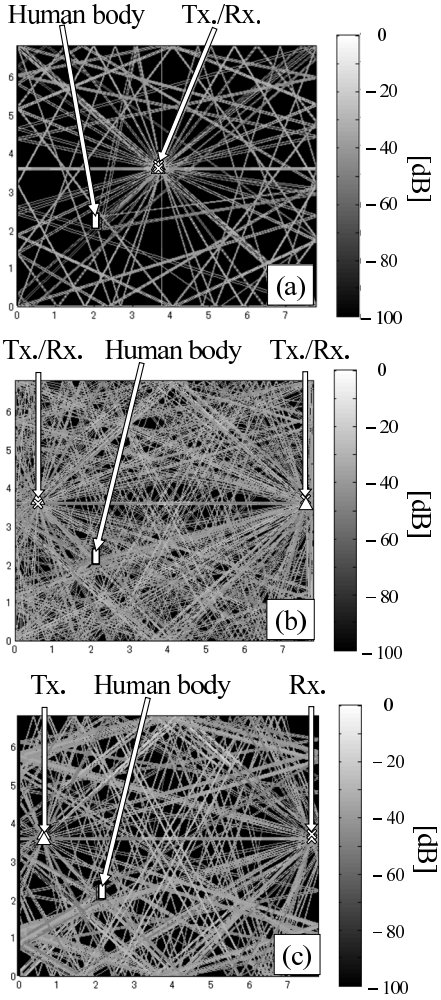

Fig. 4 Path distribution based on imaging method ($W_x \times W_y \times W_z = 7.8 \times 6.8 \times 2.5\ \mathrm{m}^3$): (a) arrangement A, (b) arrangement B, (c) arrangement C.

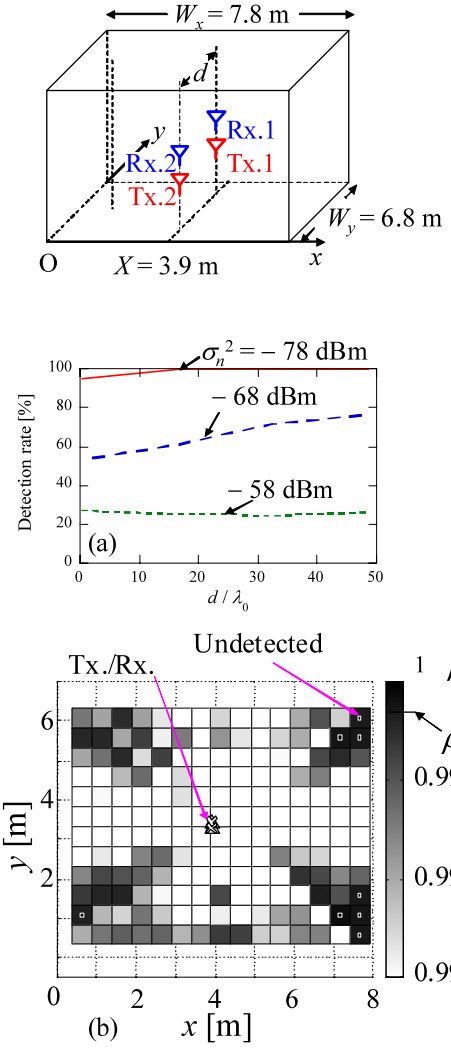

Fig. 5 Detection characteristics (arrangement A, 2.4 GHz): (a) Detection rate versus d, (b) Distribution of channel correlation.

sparse path distribution around the walls is observed. On the other hand, the arrangement B yields two kinds of paths, i.e., one is between two separated antenna sets, and another is between two closely placed transmitting and receiving antennas. Since two of them distribute totally in different ways, the sensor is expected to detect the target all over the room. Meanwhile, the path distribution in the arrangement C is relatively sparse, especially around the corners.

Figure 5(a) shows the detection rate versus the antenna spacing, d. Here, all of the antennas are located in the plane, $X = 3.9$ m, their height is 1.0 m, and d corresponds to the spacing between two sets of the transmitting and receiving antennas. The antenna location in y-axis is $Y = 3.6$ m. The transmitting power is 1 W, and the noise power is set to ${\sigma_n}^2 = -78, -68, -58$ dBm. From this result, it is found that the detection rate improves by increasing d. On the other hand, the detection rate cannot be improved even with large d when the noise power is high (${\sigma_n}^2 = -58$ dBm). This is because of the failure in the channel estimation. On the other

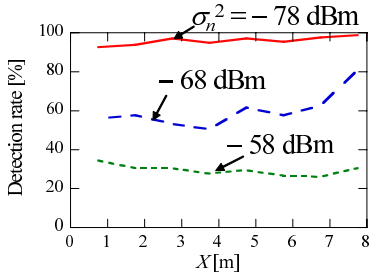

Fig. 6 Detection rate versus antenna position, X (arrangement A, $W_x \times W_y \times W_z = 7.8 \times 6.8 \times 2.5\,\mathrm{m}^3$, 2.4 GHz).

hand, more than 90% detection ratio is obtained even with small d when the noise power is sufficiently small. This indicates the proposed arrangement is effective in downsizing the antenna system.

Figure 5(b) shows the channel correlation distribution for arrangement A. Here, $d = 0.5\lambda_0$, $h = 1.0$ m, $X = 3.9$ m, $\sigma_n^2 = -78$ dBm. The antenna location in y-axis is $Y = 3.6$ m. The axes indicates the position of the human body in the room, and the intensity of ρ is shown in gray scale. The bright color means the place where the correlation is lowered by the human, and the intrusion can be easily detected at this place. On the other hand, the undetectable place is indicated by the mark, '□'. It can be found that the correlation at the location around the antenna is lowered compared to that at others. Besides, the overall value of ρ is quite high since the transmitting and receiving antennas are placed together and the strong direct paths from the transmitting antennas to receiving antennas governs the reception power. This can be understood from (3) since the varying component in the channel matrix, $\boldsymbol{H}_{ob}$ becomes small and $\boldsymbol{H}_{ob}$ approaches $\boldsymbol{H}_{no}$. In this situation, the threshold value, ρ_t, also approaches 1. The important thing is the detection is made when the power of the varying component in the channel matrix sufficiently exceeds the noise component, $\boldsymbol{H}_w$. Hence, the high correlation value does not always mean poor detection performance. Here, the threshold value of the detection was $\rho_t = 0.9999649$.

Figure 6 shows the detection rate versus the antenna location, X. Here, the spacing, d, is set to $0.5\lambda_0$, the height, d, is 1.0 m, and the antenna location in y-axis is $Y = 3.6$ m. This result shows that the detection rate is almost independent of the antenna location, X. This is because many paths exist in this environment and some of them always illuminate the human body even when the antenna is placed at the various positions. More than 90% of the detection rate is achieved when $\sigma_n^2 = -78$ dBm.

Figure 7 shows the analysis results for arrangement B. In this model, the locations of the antennas are at $X = 0.6$ m and 7.6 m, and height is $h = 1.0$ m. A set of the transmitting and receiving antennas is placed at the one side of the room and another set of the antennas is placed at another side. Here, D ($D = 7$ m) represents the distance between two sets of the antennas, and d represents the distance between the transmitting and receiving antennas in each set.

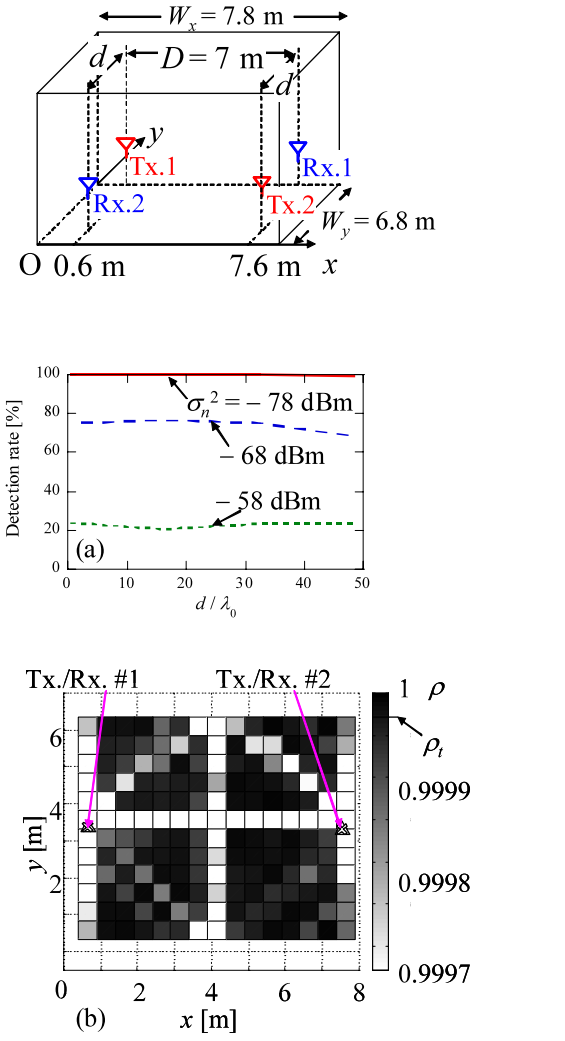

Fig. 7 Detection characteristics (arrangement B, 2.4 GHz): (a) Detection rate versus d, (b) Distribution of channel correlation.

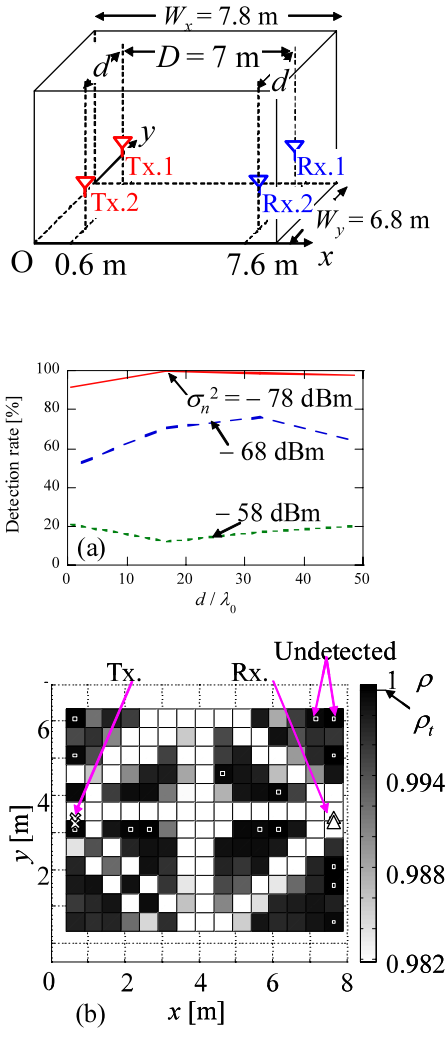

Fig. 8 Detection characteristics (conventional arrangement C, 2.4 GHz): (a) Detection rate versus d, (b) Distribution of channel correlation.

Figure 7(a) shows the detection rate versus the antenna spacing, d, where all of the simulation condition except the antenna arrangement is given identically to that in Fig. 5. Interestingly, it can be seen that the detection rate is almost independent of d. This means the antenna spacings between the transmitting antennas as well as between the receiving antennas are always around 7 m and it is sufficiently large for MIMO sensor. For $\sigma_n{}^2 = -78$ dBm, 100% of the detection rate is obtained independently of d. Even though two locations for antennas are required for arrangement B, a compact antenna configuration can be provided by making d small.

Figure 7(b) shows the channel correlation distribution for arrangement B. Here, $d = 0.5\lambda_0$, and $\sigma_n^2 = -78$ dBm. The other conditions are identical to that in Fig. 5(b). It can be seen that the correlation is greatly lowered along the lines between the Tx.1 and Rx.2. This is because the human body obstructs the direct paths. Similarly, the correlation is lowered along the once-reflected path by way of either side of the wall. As seen here, the detection is easily made when the target obstructs these strong paths. Furthermore, a large reduction in the channel correlation is observed even around the walls, like $x = 0.5, 7.5$ m. This is because of the existence of the round-trip wave between walls. Therefore, this arrangement well covers even at the corners, and the detection rate is 100% in this case. Besides, the overall correlation value is high similarly to arrangement A, since the receiving antennas have strong wave from the neighboring transmitting antennas. Here, the threshold value is set to $\rho_t = 0.9999745$.

Figure 8 represents the results of the arrangement C, i.e., the conventional one. In this case, the transmitting and receiving antennas are placed on the planes at $X = 0.6, 7.6$ m, respectively, and their height is $h = 1.0$ m. Here, the spacing between the transmitting antennas and that between receiving antennas are set to be identical, and it is represented by d. D represents the distance between two arrays, and it is set to 7 m. Figure 8(a) shows the detection rate versus the antenna spacing, d. The other parameter excluding the antenna arrangement is set to identical to the simulation

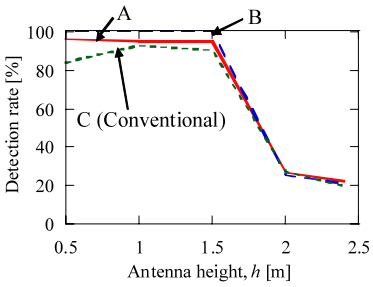

Fig. 9 Detection rate versus antenna height ($d = 0.5\lambda_0$, $\sigma_n^2 = -78$ dBm, $W_x \times W_y \times W_z = 7.8 \times 6.8 \times 2.5\,\mathrm{m}^3$, 2.4 GHz).

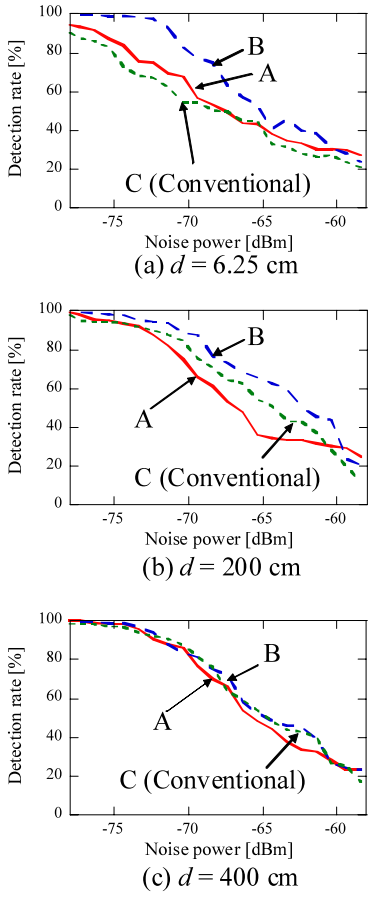

Fig. 10 Detection rate versus noise power for small room ($W_x \times W_y \times W_z = 7.8 \times 6.8 \times 2.5\,\mathrm{m}^3$, 2.4 GHz).

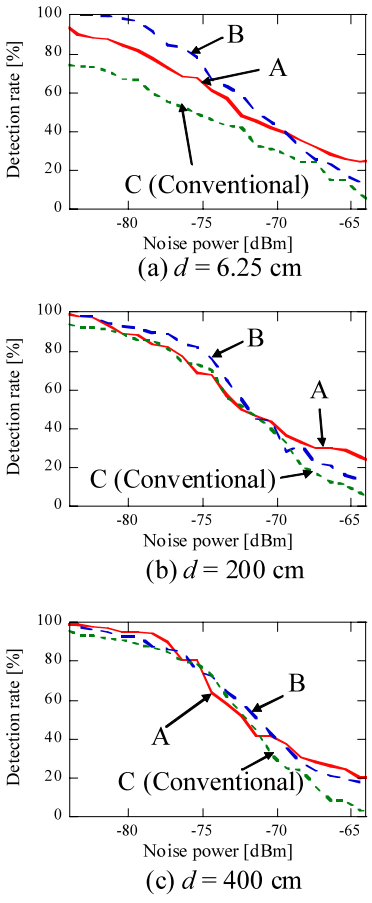

Fig. 11 Detection rate versus noise power for large room ($W_x \times W_y \times W_z = 15.6 \times 13.6 \times 2.5\,\mathrm{m}^3$, 2.4 GHz).

for the proposed arrangements A and B. From this result, it can be seen that small d yields low detection rate. When $d = 0.5\lambda_0$ and $\sigma_n{}^2 = -78$ dBm, the detection rate was 92%.

Figure 8(b) shows the distribution of the correlation coefficient of the arrangement B when $d = 0.5\lambda_0$ and $\sigma_n^2 = -78$ dBm. It is found that the bright spots appear on the direct and once-reflected paths similarly to the arrangement B. However, the undetected spots appear at the both sides of the room. This is because not so many paths distribute at the corners of the room and these areas become the dead zone. In the arrangement C, the distance between transmitting and receiving antennas is large compared with the other arrangements and this yields low SNR. The observed SNR is 25 dB and the channel correlation is $\rho_t = 0.9993874$. The correlation value tends to become lower than that in arrangements A and B, yet the threshold value also becomes low because of the low SNR. Hence, this causes the detection failures in some cases.

Figure 9 depicts the detection rate versus the antenna height. Here, the antenna spacing, d, is set to $0.5\lambda_0$, and average noise power is -78 dBm. It is clearly seen that the detection rate deteriorates when the antenna is higher than human body, whose height is 1.7 m. This tendency is observed in all three arrangements, and it is found that the antenna needs to be located lower than the height of the human body.

The detection rates versus the noise power with various antenna spacings are evaluated for two sizes of the room. Figures 10 and 11 indicate the detection rate for small and large rooms, respectively. Also, the results (a), (b), and (c) correspond to the antenna spacings, 6.25, 200, and 400 cm, respectively. From these results, it can be seen that the arrangement B yields the highest detection rate in most cases. The detection rate of the arrangement B with $d = 6.25$ cm is comparable to that of the arrangement C with $d = 400$ cm

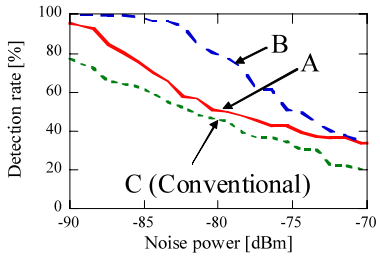

(a) $d = 6.25$ cm

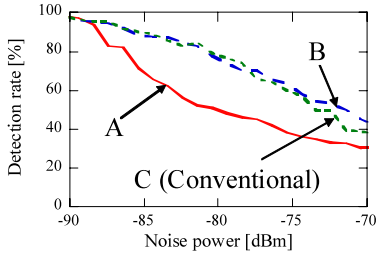

(b) $d = 200$ cm

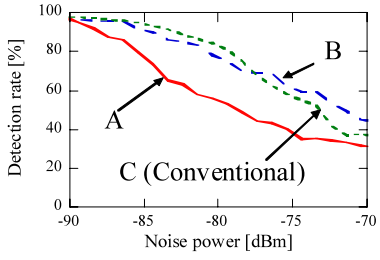

(c) $d = 400$ cm

Fig. 12 Detection rate versus noise power for small room ($W_x \times W_y \times W_z = 7.8 \times 6.8 \times 2.5\,\mathrm{m}^3$, 5.2 GHz).

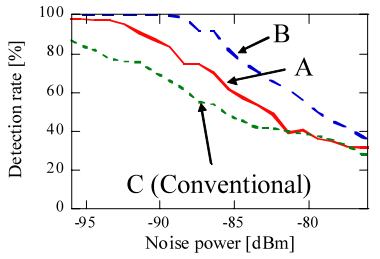

(a) $d = 6.25$ cm

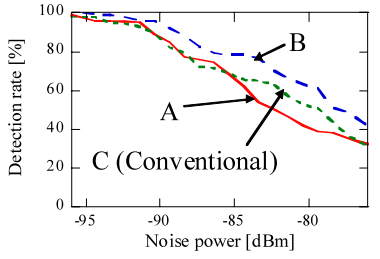

(b) $d = 200$ cm

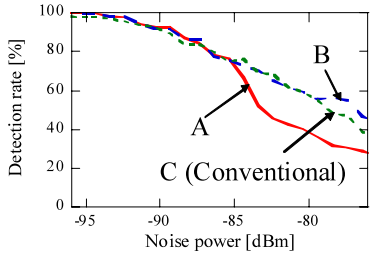

(c) $d = 400$ cm

Fig. 13 Detection rate versus noise power for large room ($W_x \times W_y \times W_z = 15.6 \times 13.6 \times 2.5\,\mathrm{m}^3$, 5.2 GHz).

for both room sizes. Even though the detection rate of the arrangement A is lower than that of B, the arrangement A achieves the detection rate as high as the arrangement C, and offers the smallest size of the antenna. It is also found that the MIMO sensor at the large room requires small noise power and this comes from the low reception power caused by the large path loss. The required noise level at the large room is lower by approximately 6 dB than that at the small room in this case.

The effect of the frequency on the detection performance is evaluated to consider the feasibility of the proposed antenna arrangements. Figures 12 and 13 show the detection rates for two types of the rooms when the frequency is set to 5.2 GHz. Here, the results (a), (b), and (c) correspond to the antenna spacings, 6.25, 200, and 400 cm, respectively. Even though the frequency is much higher than that in Figs. 10 and 11, very similar tendency in the detection characteristics is observed. However, the required noise level is about 7–10 dB lower than that for 2.4 GHz. This is because of the large path loss at 5.2 GHz. Nevertheless, the arrangement B yields almost equal or higher detection ratio than arrangement C does for both room sizes. Though the detection ratio of the arrangement A is lower than the others when the antenna spacing, d, is large, the detection ratio comparable to the others can be attained when $d = 6.25$ cm. It is considered that the distributed antenna arrangement, i.e. method B, is suitable for the situation where the path loss is large.

5. Conclusion

In this paper, the antenna arrangements for the MIMO sensor have been proposed. In these arrangements, the transmitting and receiving antennas are placed together. The numerical analysis of the indoor propagation based on the ray-tracing method is carried out. The intrusion detection performance with the various antenna arrangements are evaluated for the human positions all over the room. The numerical analysis results showed that the proposed arrangements can achieve comparable or higher detection rate than the conventional arrangement when the antenna spacing is limited. Especially, the detection rate of the proposed arrangement B is equal or superior to that of the conventional arrangement with large antenna spacing, such as 400 cm, even when the antenna spacing is 6.25 cm. This tendency is observed even for the situation, where the frequency is high or the room size is large. From these results, it is found that two proposed antenna arrangements are effective in down-

sizing the antenna configurations of MIMO sensor without paying any cost of the detection rate.

Acknowledgments

This work is supported in part by the Center for Revitalization Promotion of the Japan Science and Technology Agency (JST), and JSPS KAKENHI (23500549).

References

[1] A. Hatami and K. Pahlavan, "In-building intruder detection for WLAN access," IEEE Pos., Loc. and Nav. Symp., pp.592–595, April 2004.
[2] M. Nishi, S. Takahashi, and T. Yoshida, "Indoor human detection systems using VHF-FM and UHF-TV Broadcasting waves," Proc. 2006 IEEE Int. Symp. Personal Indoor Mobile Radio Commun. (PIMRC'06), Sept. 2006.
[3] Y. Okugawa, Y. Akiyama, H. Yamane, and K Tajima, "Study on an intrusion detecting method using TV broadcasting waves," Proc. of 2007 Int. Symp. Antenna Propagat. (ISAP 2007), Nov. 2007.
[4] S. Ikeda, H. Tsuji, and T. Ohtsuki, "Indoor event detection with signal subspace spanned by eigenvector for home or office security," IEICE Trans. Commun., vol.E92-B, no.7, pp.2406–2412, July 2009.
[5] N. Honma, T. Sugiura, K. Nishimori, H. Sato, and Y. Tsunekawa, "MIMO sensor — Experimental channel characterization in indoor environment," Proc. 2010 Int. Symp. Antenna Propagat. (ISAP 2010), Nov. 2010.
[6] K. Nishimori, Y. Koide, N. Honma D. Kuwahara, H. Yamada, and H. Makino, "MIMO Sensor — Effectiveness of distributed MIMO antenna configuration," Proc. 2010 Int. Symp. Antenna Propagat. (ISAP 2010), Nov. 2010.
[7] K. Nishimori, Y. Koide, D. Kuwahara, N. Honma, H. Yamada, and H. Makino, "MIMO sensor — Evaluation on antenna arrangement," 5th European Conf. Antennas and Propagat. (EuCAP 2011), Electric Proc. EuCAP 2011, April 2011.
[8] K. Nishimori, K. Ushiki, and N. Honma, "Experimental evaluation toward transmit and receive diversity effect in SIMO/MIMO sensors," 6th European Conf. Antennas and Propagat. (EuCAP 2012), Electric Proc. EuCAP 2012, Post2-30, March 2012.
[9] A. Kumakura, H. Yamada, K. Nishimori, and Y. Yamaguchi, "Fundamental study on channel model of MIMO sensor for event detection," Proc. 2011 Int. Symp. Antenna Propagat. (ISAP 2011), Oct. 2011.
[10] N. Honma, K. Nishimori, H. Sato, and Y. Tsunekawa, "Compact antenna arrangement for MIMO sensor in indoor environment," Proc. 2012 Int. Symp. Antenna Propagat. (ISAP 2012), Nov. 2012.

Naoki Honma received the B.E., M.E., and Ph.D. degrees in electrical engineering from Tohoku University, Sendai, Japan in 1996, 1998, and 2005, respectively. In 1998, he joined the NTT Radio Communication Systems Laboratories, Nippon Telegraph and Telephone Corporation (NTT), in Japan. He is now working for Iwate University. He received the Young Engineers Award from the IEICE of Japan in 2003, the APMC Best Paper Award in 2003, and the Best Paper Award of IEICE Communication Society in 2006, respectively. His current research interest is planar antennas for high-speed wireless communication systems. He is a member of IEEE.

Kentaro Nishimori received the B.E., M.E., and Dr.Eng. degrees in electrical and computer engineering from Nagoya Institute of Technology, Aichi, in 1994, 1996, and 2002, respectively. He joined NTT Wireless Systems Laboratories in 1996. He was a visiting researcher at the Center for TeleInFrastruktur, Aalborg University, Denmark in 2006. He received the Young Engineers Award from the Institute of Electronics, Information and Communication Engineers (IEICE) of Japan in 2001 and Young Engineer Award from IEEE AP-S Japan Chapter in 2001. His current research interests are multi-user MIMO systems and cognitive radio systems. He is a member of IEEE.

Hiroaki Sato received the B.E. degree in electronic engineering from Utsunomiya University, Utsunomiya, Japan, in 1990 and the M.E. and Ph.D. degrees in electrical and communication engineering from Tohoku University, Sendai, Japan, in 1992 and 1995, respectively. In 1995, he joined ONO SOKKI CO., LTD., Yokohama, Japan. Since 2002, he has been with the Faculty of Engineering, Iwate University. His current research interests include digital signal processing and digital system control. He is a member of the Institute of Electronics, Information and Communication Engineers of Japan.

Yoshitaka Tsunekawa received the B.E. degree from Iwate University, Morioka, Japan, in 1980 and the M.E. and the Doctor of Engineering degrees from Tohoku University, Sendai, Japan, in 1983 and 1993, respectively. Since 1983, he has been with the Faculty of Engineering, Iwate University, where he is now a professor at the Department of Electrical Engineering and Computer Science. His current research interests include digital signal processing and digital control. He is a member of the Institute of Electronics, Information and Communication Engineers of Japan, and IEEE.